Bioelectrochemistry 74 (2008) 142–148

Contents lists available at ScienceDirect

Bioelectrochemistry

journal homepage: www.elsevier.com/locate/bioelechem

Interfacial electron transfer on cytochrome-*c* sensitised conformally coated mesoporous TiO_2 films

Emmanuel Topoglidis [a,*], Thierry Lutz [a,1], James R. Durrant [a], Emilio Palomares [b,c,*]

[a] Center of Electronic Materials and Devices, Department of Chemistry, Imperial College, Exhibition Road, London SW7 2AY, United Kingdom
[b] Institute of Chemical Research of Catalonia (ICIQ), Avda. Països Catalans, 16. Tarragona, C.P. 43007 Tarragona, Spain
[c] Institucio Catalana de Recerva i Estudis Avancats (ICREA). Passeig Lluis Companys, 23. E-08010 Barcelona, Spain

ARTICLE INFO

Article history:
Received 13 February 2008
Received in revised form 14 May 2008
Accepted 11 June 2008
Available online 21 June 2008

Keywords:
Cytochrome-*c*
Metal oxide coatings
Bioelectrochemistry
Conductivity
TiO_2 films

ABSTRACT

Hybrid protein films incorporating Cyt-*c* immobilized on TiO_2 films were prepared and characterised optically with UV–visible spectroscopy and electrochemically with cyclic voltammetry, and their conductivity properties were studied in detail. In addition the effects of a thin overlayer coating of a second metal oxide such as SiO_2, Al_2O_3, ZrO_2 and MgO_2 were studied and the effects over the electrochemical properties of the hybrid working electrodes were discussed.

1. Introduction

Mesoporous nanocrystalline TiO_2 electrode is a wide-band-gap (~3 eV) semiconductor and therefore optically transparent for wavelengths ≤390 nm. The thin transparent films comprise a rigid, porous network of 10–20 nm nanocrystalline TiO_2 nanoparticles with pore sizes between 5 and 20 nm, sufficiently large for proteins to diffuse throughout the porous structure. The surface area of such films is greatly enhanced over flat electrode surfaces (up to 1000 fold for an 8-μm-thick film). In addition to their optical transparency and high surface area, these films exhibit good stability, and electrochemical activity at potentials above the conduction band edge.

We have previously demonstrated that protein adsorption can be readily achieved on mesoporous TiO_2 electrodes from aqueous solutions at 4 °C with high binding stability and undetectable protein denaturation [1–5]. We have characterized the properties of such protein/TiO_2 electrodes by cyclic voltammetry and UV–visible spectroscopy and demonstrated that the immobilized proteins can be reduced by the application of an electrical potential to the film without the addition of any electron-transfer mediators [1–5]. Moreover, other groups have also shown the adsorption of a range of biomolecules on mesoporous metal oxide electrodes as working electrodes for sensing devices [6–15].

In this paper we aim to examine further the conductivity and electrochemical properties of these electrodes as a function of pH and scan rate by using a simple solution phase redox system such as $Fe(CN)_6$. Both cyclic voltammetry (CV) and spectroelectrochemistry will be used. In addition, the electrochemical behaviour of Cyt-*c* will be studied on TiO_2 films with a thin conformally deposited overlayer of a second metal oxide such as SiO_2, Al_2O_3, ZrO_2, and MgO_2. The effect on the interfacial electron-transfer process between the electrode and the biomolecules is studied.

2. Experimental section

2.1. Reagents

Horse-heart cytochrome-*c* was purchased from Sigma Chemical Co and Carbowax 20,000 from Fluka. Silicon Methoxide (99.9%), Alumina tri-*sec*-butoxide (99.9%), Zirconia *iso*-butoxide (99.9%), Magnesium ethoxide (99.9%), and the remaining chemicals were purchased from Aldrich Chemical Co. and used as received. Sodium dihydrogen orthophosphate (0.01 M) was used to prepare the supporting electrolyte, and its pH was adjusted to 7 using NaOH. Distilled water was demineralised to a resistivity of 10 MW cm^{-1}. Fluorine-doped tin oxide-coated glass slides (conductivity of 15 W cm^{-2}) were purchased from Hartford Glass (Hartford City, Indiana, U.S.A.), cleaned with water, rinsed with ethanol, dried at 100 °C and heated at 450 °C prior to film deposition.

* Corresponding authors. Topoglidis is to be contacted at Acrongenomics Inc., 14 Rue Kleberg, CH-1201, Geneva, Switzerland. Tel.: +41 22 7165300; fax: + 41 22 7165319.
E-mail address: manosphd@yahoo.com (E. Topoglidis).
[1] Present address: Advanced Technology Institute, School of Electronics & Physical Sciences, University of Surrey, GU2 7XH, United Kingdom.

1567-5394/$ – see front matter © 2008 Elsevier B.V. All rights reserved.
doi:10.1016/j.bioelechem.2008.06.006

2.2. Preparation of electrodes

The TiO_2 paste, consisting of 15 nm sized particles was prepared from a sol–gel colloidal suspension containing 12.5 wt.% TiO_2 particles and 6.2 wt.% Carbowax 20,000 as reported previously [16]. The TiO_2 suspension was then applied to the surface of the conducting glass using the "doctor blade" technique. Masking the glass slide with Scotch tape controlled the thickness and the width of the area spread, with one layer of tape being employed to yield a final film thickness of 4 μm. The spread suspension was then allowed to dry before being sintered for 20 min at 450 °C. The thickness of the nanocrystalline TiO_2 films was measured with a DEKTAK profilometer. The TiO_2 films were cut in 1 cm^2 pieces. Immediately prior to Cyt-*c* immobilization, the films were heated to 450 °C for 15 min and then allowed to cool down to room temperature before being immersed in the protein solution.

2.3. Coating procedure

To achieve uniform coating of the preformed nanocrystalline mesoporous TiO_2 thin film we have used a previously described method [17]. In brief, the conformally coating of the different metal oxides were obtained by in-situ hydrolysis of the alkoxide precursors over the nanoparticles. The highly hydroxilated surface of the mesoporous thin films induces the formation of nanoscopic thin uniform layers of the corresponding metal oxide on the surface of the nanocrystalline particle. The precursor solutions concentrations used were 0.15 M for aluminium tri-*sec*-butoxide in dry 2-propanol, 0.15 M for silicon methoxide in dry methanol, 0.15 M for zirconium *iso*-butoxide in dry methanol and 0.15 M for magnesium ethoxide in dry methanol. These non-scattering precursor solutions were prepared under anaerobic conditions in a glovebox; however, once prepared the solutions were not air sensitive, allowing dipping to be conducted in ambient conditions.

After their initial sintering, the TiO_2 films were coated with metal oxides overlayers by dipping each film in a solution of the suitable precursor pre-heated to 60–70 °C, for 20 min, followed by heating at 435 °C for 20 min [17]. To keep similar conditions between the standard and coated electrodes, the mesoporous TiO_2 films without coatings were sintered at the same time as coated ones.

Experiments were conducted as a function of precursor concentration, dipping time and temperature and number of dipping/sintering cycles. The overlayer growth was found to be insensitive to dipping time or temperature, but dependent upon precursor concentration and the number of repeat cycles, consistent with previous observations [17]. For convenience, the precursor concentration was maintained at 0.15 M for all studies reported in this paper, with the overlayer thickness being controlled only by repeating the dipping/sintering cycle up to 4 times.

2.4. Protein immobilization

The protein immobilization was achieved by the immersion of 1 cm^2 pieces of TiO_2 (coated or uncoated) films in 2 ml of the protein solution (20 μM Cyt-*c* in a 10 mM phosphate buffer) at 4 °C for at least 1 to 2 days. Cyt-*c* adsorption onto the films was monitored by recording the UV–Vis absorption spectra of the films at room temperature.

2.5. Optical measurements

All absorption spectra were measured using a Shimadzu UV-2401 spectrophotometer with a sampling interval of 1 nm. Protein solutions were measured in the appropriate buffered solution, that was also used for the blank spectra, using plastic rather than quartz cuvettes in order to prevent the binding of protein molecules during the acquisition. During the Cyt-*c*/TiO_2 film analysis, the sensitised films were submerged in the buffer solution. Prior to all spectroscopic measurements, the films were removed from the immobilization solution and rinsed in a buffer solution to remove non-immobilized protein. Contributions to the spectra from scatter and absorption by the TiO_2 film were subtracted by using protein-free reference films.

2.6. Electrochemical measurements

The electrochemistry and spectroelectrochemical experiments were carried out using an Autolab PGStat12 potentiostat and a three-electrode cell with quartz windows, a platinum mesh flag as the counter electrode, a Ag/AgCl in 3.5 M KCl reference electrode, and the TiO_2 or Cyt-*c*/TiO_2 film on conducting glass as the working electrode. The electrolyte, an aqueous solution of 10 mM sodium phosphate (pH 7), was thoroughly degassed by bubbling argon prior to the experiments. For the spectroelectrochemical experiments, the above cell was incorporated as a sample in the Shimadzu UV-1601 spectrophotometer, and the absorption changes were monitored as a function of the applied potential. All potentials are reported against the Ag/AgCl electrode and an argon blanket was maintained during all measurements.

3. Results

3.1. Electrochemical studies

We have previously demonstrated that CV can be used to study the electrochemical behaviour of immobilized proteins such as Cyt-*c* on the mesoporous TiO_2 films [1–5]. CV is a useful technique to examine the redox electrochemistry between the TiO_2 electrode and the immobilized Cyt-*c*. From these studies, we concluded that the negative shift between the observed reduction peaks from the CVs of the immobilized Cyt-*c* on mesoporous TiO_2 films and the ones observed in solution can be attributed to the low conductivity of TiO_2 films [18] at moderate potentials or due to a shift in the redox potential of Cyt-*c* induced by its immobilization [3–5].

To lift this uncertainty, a number of control experiments have been conducted in this paper to further understand the interfacial electron-transfer reactions between the mesoporous semiconductor film and the Cyt-*c*. Using a simple solution phase redox couple such as potassium ferricyanide, $K_3[Fe(CN)_6]$ and an unmodified mesoporous TiO_2 film as a working electrode we obtained the CV shown in Fig. 1A. Although potassium ferricyanide is not immobilized on the TiO_2 film, a negative shift in its reduction peak, identical to the one observed with the Cyt-*c*, occurs. This was also confirmed by a control experiment in which a TiO_2 film is dipped into a $K_3[Fe(CN)_6]$ solution, taken out and washed thoroughly, and then subjected to CV in pure phosphate buffer solution and no characteristic Fe redox peak was obtained (results not shown here). Thus we can conclude that the voltammetry is dominated by the conductive properties of the TiO_2 film.

We did also examine the effect of the scan rate on the CV. Slower scan rates were applied to the Cyt-*c*/TiO_2 electrode in order to try to obtain a reversible peak shaped CV. Fig. 2 illustrates that even at slow scan rates no simple reversible behaviour for the Cyt-*c*/TiO_2 film was observed, consistent with the currents being limited by the low TiO_2 conductivity at moderate potentials.

It is known that the pH of the electrolyte solution affects the conductivity of the TiO_2 films. Indeed, the change in pH, by simply altering the $HPO_4^{2-}/H_2PO_4^-$ ratio but keeping the ionic strength constant, has a significant effect on the potential of the reduction peak for the immobilized Cyt-*c* as can be seen in Fig. 3. The CVs of this figure show that by lowering the pH by 1 unit, the potential of the reduction peak of Cyt-*c* changes by 64.5 mV due to the change in the conductivity of the TiO_2 films. These results are in agreement with the fact that a blank nanocrystalline TiO_2 film in an aqueous electrolyte shows an expected Nernstian shift of ~59.1 mV on increasing the pH of

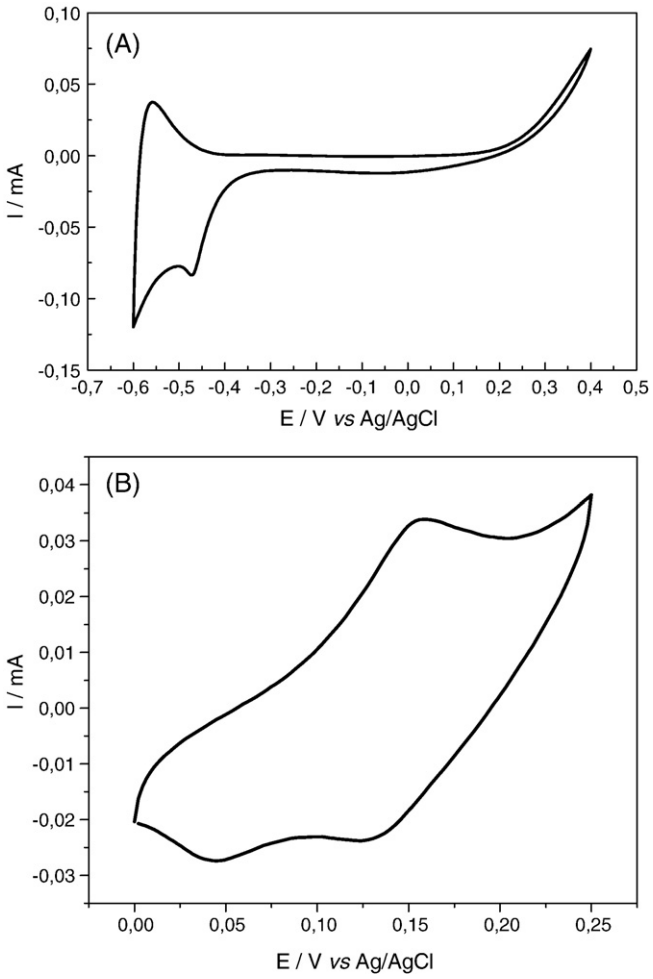

Fig. 1. (A) CV for a blank TiO_2 film in $Fe(CN)_6$ solution. (B) The normal behaviour of $Fe(CN)_6$ in solution.

the electrolyte by a single unit [19–20]. This supports the assignment of the shift of the reduction peak of the immobilized proteins to the conductivity of the TiO_2 film.

3.2. Spectroelectrochemical studies of blank TiO_2 films

In order to further examine the conductivity of the TiO_2 films spectroelectrochemical techniques were used. These techniques take advantage of the facts that thin nanostructured TiO_2 films may be deposited on conducting glass supports to yield transparent electrodes and that electrons present in these electrodes have an optical spectroscopy characteristic of their local environment. Following the procedure of [18] spectroelectrochemical data was collected using 10 mM NaH_2PO_4 (pH 7) as the electrolyte for blank TiO_2 films. The results are shown in Fig. 4A: at low and moderate negative applied potentials the measured absorption spectra is pretty much the same as the one for which no potential is applied. At still more negative potentials, however, a broad absorption maximum is observed at about 750 nm.

Fig. 4B follows the absorption increase at a single wavelength (750 nm) as a function of the applied bias. Although the increase in absorbance is higher the more negative the potential applied, the kinetics of these increases are the same (10–15 s).

It has been suggested that the coloration (blue/black) of the TiO_2 film under negative applies bias is due to the filling of the trap/conduction band states [18,19]. Therefore the change in absorbance at 750 nm can be related to the electron density per nanoparticle, n. The

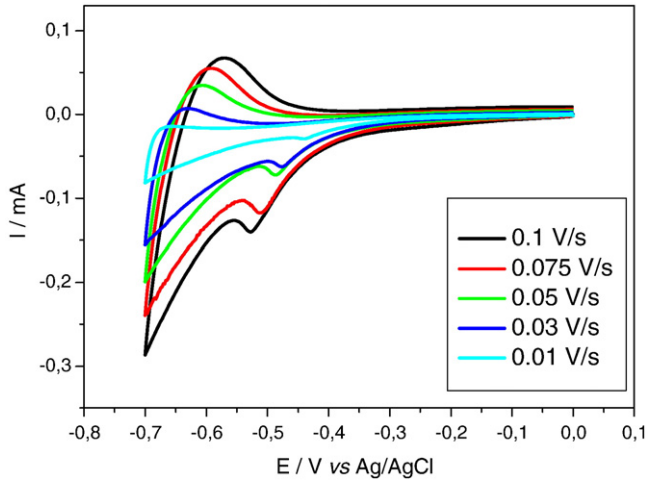

Fig. 2. Cyclic voltammograms for a Cyt-c/TiO_2 film in a pH 7, 10 mM NaH_2PO_4 buffer at different scan rates (V/s).

electron density can thus be determined from the spectroelectrochemical data by monitoring the increase in absorption at 750 nm as a function of externally applied bias. The change in absorbance A is defined by the Beer–Lambert law:

$$A = \varepsilon c l \tag{1}$$

Where ε is the extinction coefficient of an electron at 800 nm, 1.3×10^{-21} m^2 [18], c is the concentration and l the path length. Eq. (1) can be used to derive the electron density n per nanoparticle by substituting c with n/V. This is given by the Eq. (2).

$$n = \frac{AV}{\varepsilon l} \tag{2}$$

where V is the volume of the TiO_2 film, 8×10^{-10} m^3 and l is the thickness of the TiO_2 film, 8×10^{-6} m and n is the electron density. It is estimated that there are 2.25×10^{14} nanoparticles in a film volume of 8×10^{-10} m^3 assuming 15 nm sized particles in an 8 μm thick film. The results are shown in Fig. 5.

From this graph, it is obvious that the data exhibit an approximately exponential tail towards the more positive biases. It has been suggested that this tail may be due to the presence of sub-band gap defect states [18]. At −0.3 V the electrons start filling the trap/conduction band states of the blank TiO_2 film at a rate of 0.1 e^- per

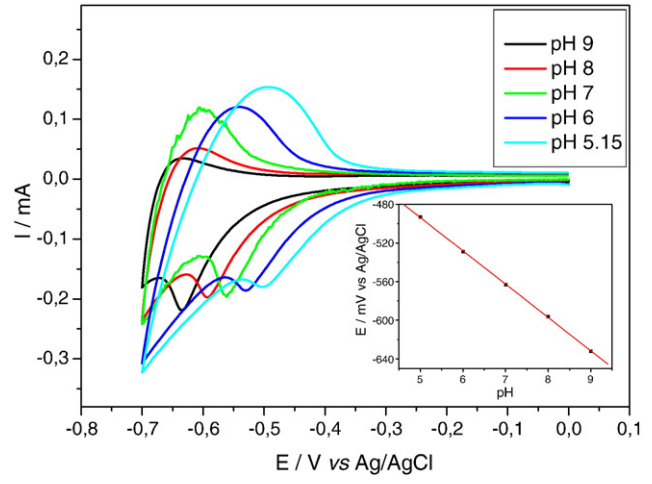

Fig. 3. CVs for Cyt-c/TiO_2 at different pHs, at scan rate 0.1 V/s.

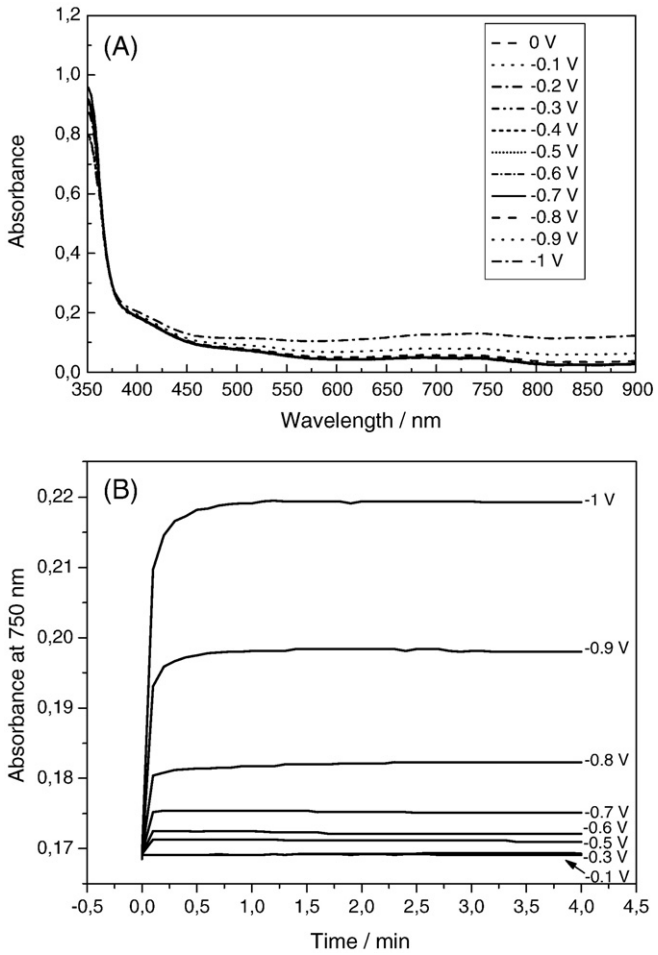

Fig. 4. Spectroelectrochemical data showing (A) the absorption spectrum of a blank TiO_2 electrode in 10 mM phosphate buffer solution, pH 7, measured at 0 to −1 V *vs* Ag/AgCl reference electrode. (B) The time dependent absorbance changes at 750 nm for a blank TiO_2 electrode measured at measured at −0.1 to −1 V *vs* Ag/AgCl reference electrode.

nanoparticle. This rate increases as the negative applied potential is increased reaching a value of 17.5 e^- per nanoparticle at −1 V. Therefore, these results confirm the limited conductivity through the TiO_2 films at low potentials.

The same spectroelectrochemical experiments were performed on Cyt-*c*/TiO_2 films. From Fig. 6 it is obvious that the reduction rate of the adsorbed Cyt-*c* is consistent with the conduction these films show. At

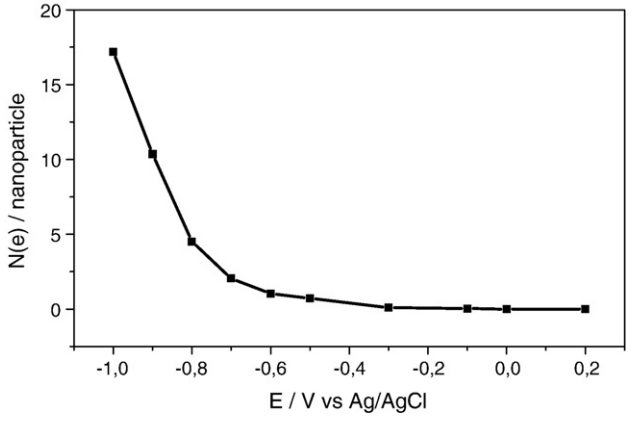

Fig. 5. Electron density in a blank TiO_2 electrode as a function of bias.

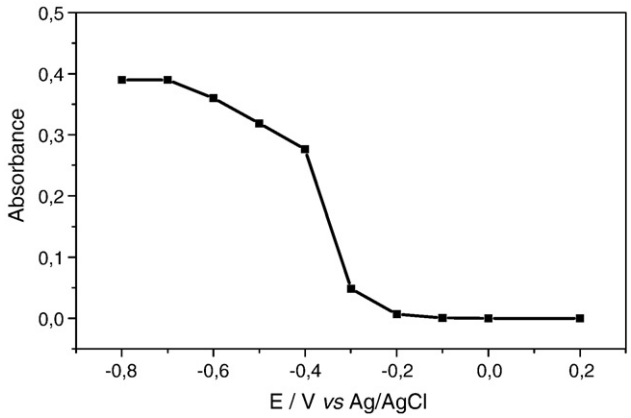

Fig. 6. Optical absorbance at 550 nm for Cyt-*c*/TiO_2 measured as a function of the applied potential. Each potential step was applied for 15 min before the absorbance was recorded.

low biases (0 to −0.3 V) there is no conduction occurring and therefore the adsorbed Cyt-*c* remains in its Fe^{3+} oxidation state. At biases higher than −0.3 V Cyt-*c* starts getting reduced to its Fe^{2+} state and the amount of Cyt-*c* reduction increases as the negative applied bias is increased reaching saturation (all the adsorbed Cyt-*c* is reduced) at −0.7 V. Therefore it is concluded that the reduction kinetics of the adsorbed Cyt-*c* pretty much matches the increase in Ti^{3+} absorbance measured with no protein molecules adsorbed on the films.

3.3. Effect of coatings on the conductivity of the TiO_2 films

The electrochemical properties of Cyt-*c* on TiO_2 electrodes coated with an overlayer of either SiO_2, ZrO_2, Al_2O_3 or MgO_2 was investigated, as for an unmodified TiO_2 electrode, by incorporating the films as the working electrode of a three-electrode photoelectrochemical cell. The fraction (%) of the immobilized Cyt-*c* reduced as a function of the applied bias on each coated film was determined by potential step chronoamperometry as shown in Fig. 7A and B. An example of these measurements is given in Fig. 8 for Cyt-*c* immobilized on TiO_2 film coated with SiO_2. As the applied potential increases, a clear shift in the Soret band from 410 to 416 nm and an increase in the sharp α and β bands at 550 and 520 nm are observed, in good accordance with the solution spectrum of the reduced Cyt-*c* [22]. Each UV–vis spectrum was taken 15 min after applying a step potential to ensure the redox couple reach equilibrium. For all overlayers, complete (90%) reduction of the immobilized Cyt-*c* is observed, indicating that all of the adsorbed protein is electroactive.

The fraction of Cyt-*c* reduced as a function of potential and oxide overlayer, determined from the relevant spectroelectrochemical data (as shown for Cyt-*c*/SiO_2–TiO_2 in Fig. 8), is shown in Fig. 7B. It is apparent that the bias dependence of the amount of protein reduced is strongly dependent upon nature of the overlayer.

Thus, our spectroscopic studies confirmed that the application of a potential more negative than −0.1 and −0.3 V *vs* Ag/AgCl to the conducting glass substrate of the Cyt-*c*/TiO_2 and Cyt-*c*/SiO_2–TiO_2 electrodes, respectively, resulted in the reduction of the Fe(III) heme moiety of Cyt-*c* to Fe(II). Similarly, potentials more negative than −0.3, −0.5 and −1 V were necessary for the reduction of Cyt-*c* on TiO_2 films coated with either ZrO_2, Al_2O_3 or MgO_2 respectively.

According to Fig. 8 the half wave potential ($E_{1/2}$) for the Cyt-*c*/TiO_2 and Cyt-*c*/SiO_2-TiO_2 films are −0.46 and −0.33 V *vs* Ag/AgCl, respectively. The mid-point potentials of Cyt-*c* for the rest of the ovelayers are shown on Table 1. For all the TiO_2 coated with overlayers, re-oxidation of the immobilized Cyt-*c* could be achieved by bubbling the buffer solution with oxygen, by adding a chemical oxidant such as potassium ferricyanide or by the prolonged application of a positive

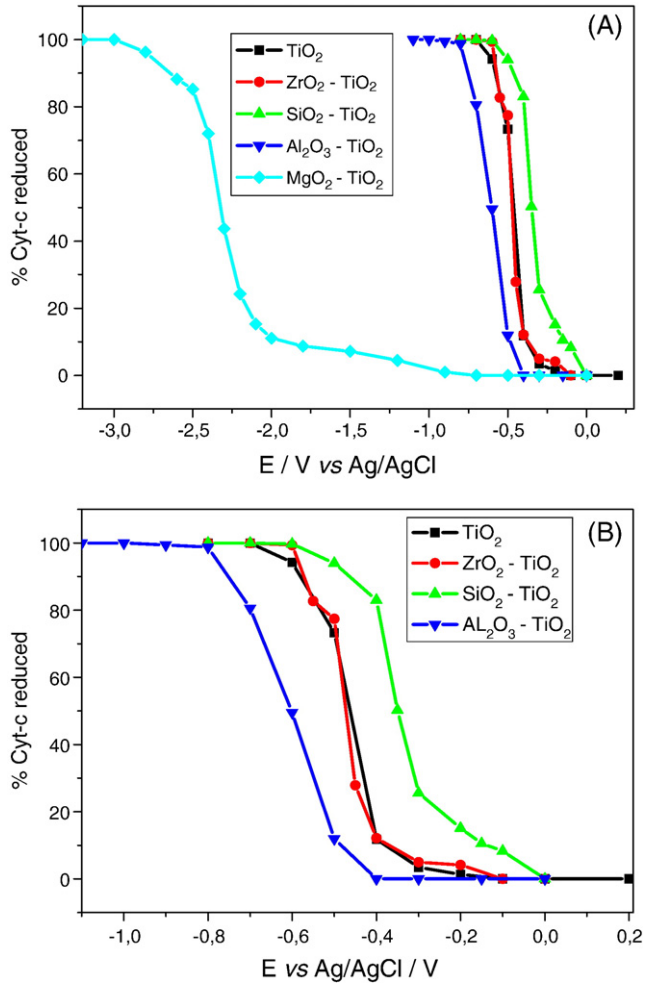

Fig. 7. (A) Percentage of Cyt-*c* reduced on TiO_2 films coated with either Silica or Zirconia or Alumina or Magnesium, as a function of the applied potential determined from the relative spectroelectrochemical data. Each potential was applied for 15 min before the absorbance at 550 nm was recorded. (B) Percentage of Cyt-*c* reduced on TiO_2 films coated with either Silica or Zirconia or Alumina.

potential (e.g. 0.6 V *vs* Ag/AgCl) whilst bubbling with argon. However, the latter, electrochemical reoxidiation was relatively slow ($t_{1/2}$ ~4 to 120 min depending on the film, fastest for the SiO_2 overlayer and slowest for the Au overlayer), consistent with the very low conductivity of all films at such positive potentials.

Table 1
Characteristics of the metal oxide overlayers [23] employed in this study compared with uncoated TiO_2 films

Metal oxide overlayer	Band gap [eV]	PZC (pH units)	$E_{1/2}$ of immobilized Cyt-*c* [V]
SiO_2	8.0–8.90	2.10	−0.33
ZrO_2	5.0	5.10	−0.46
Al_2O_3	8.45–9.90	9.20	−0.62
MgO_2	7.6–7.75	8.90	−2.20
TiO_2	3.0–3.30	5.50	−0.45

The spectroelectrochemical studies reported in Figs. 7 and 8 were further supported by CV studies of these coated and uncoated TiO_2 films. All cyclic voltammetry experiments were carried out in a protein-free, anaerobic 0.01 M phosphate buffer solution of pH 7. As stated previously and in other papers [4,14], control cyclic voltammograms (CVs) of protein-free 4-μm thick coated and uncoated TiO_2 films show the characteristic charging/decharging currents assigned to electron injection into sub-band gap/conduction band states of the TiO_2 films. In all cases the CVs integrate to approximately 0, indicating negligible Faradic currents. The charging of the TiO_2 film coated with a SiO_2 overlayer starts earlier than the one of the uncoated TiO_2 film as shown in Fig. 9 whilst in the case of zirconia, the film charging starts almost at the same bias as in the uncoated case. Finally, it is worth noting that the amount of charge one can inject into the film in our experiments was observed to be less for the Al_2O_3 coated films and least for the MgO_2 coated films.

Fig. 10 shows the CVs of Cyt-*c* immobilized on uncoated and SiO_2 coated TiO_2 films. These CVs show, in addition to the charging/discharging currents observed for the bare films, reduction peaks for Cyt-*c* at −0.58 and −0.48 V, respectively. These reduction peaks are in reasonable agreement with the mid-point redox potentials of the spectroelectrochemical data (shown in Figs. 7 and 8) supporting the assignment of these peaks specifically to Cyt-*c* reduction.

No additional oxidative peaks in the reverse scans can be observed for either Cyt-*c*/TiO_2 or Cyt-*c*/ SiO_2–TiO_2 films. The solution phase oxidation potential for Cyt-*c* is 38 mV *vs* Ag/AgCl [24]. The absence of any Cyt-*c* oxidation peak in the voltammograms is consistent with the very limited conductivity of either film for potentials greater than 38 mV. The negative shift of the reduction peaks relative to the solution mid-point potential is attributed to the limited conductivity

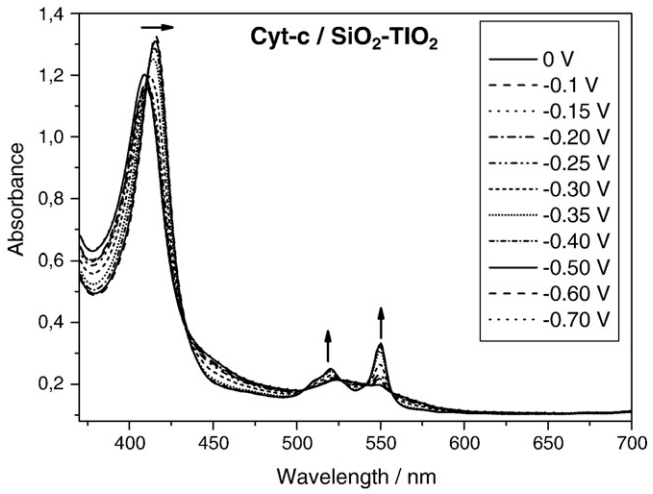

Fig. 8. UV–vis absorption spectra for electrochemical reduction of the oxidised Fe(III) Cyt-*c* immobilised on a mesoporous TiO_2 coated with silica at increasing negative potentials (0 to −0.7 V *vs* Ag/AgCl).

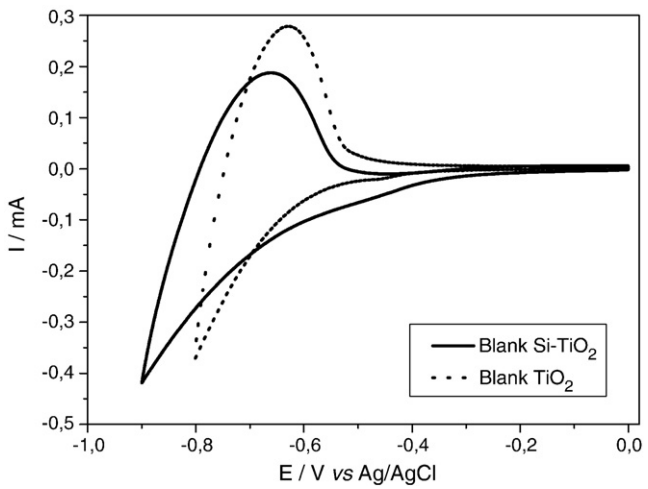

Fig. 9. CVs at 0.1 V s^{-1} in a pH 7, 10 mM NaH_2PO_4 buffer for a mesoporous TiO_2 film and a mesoporous TiO_2 coated with silica.

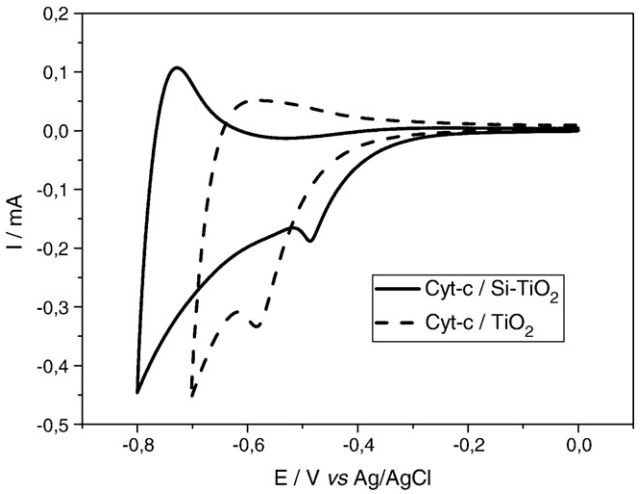

Fig. 10. CVs at 0.1 V s^{-1} in a pH 7, 10 mM NaH_2PO_4 buffer for Cyt-*c*/TiO_2 film and a Cyt-*c*/TiO_2 coated with silica.

of the metal oxide films over this potential range. The 100 mV positive shift of the reduction peak observed for the Cyt-*c*/SiO_2–TiO_2 film relative to the Cyt-*c*/TiO_2 film is consistent with the greater conductivity of the SiO_2–TiO_2 films, as indicated by the 200 mV shift in the control voltammograms shown in Fig. 9.

4. Discussion

The voltammogram of a Cyt-*c*/TiO_2 film shows irreversible electron transfer from the TiO_2 film to the protein above a threshold of ~−0.3 V [4]. This is a substantially more negative value for Cyt-*c* reduction than would be expected on the basis of its solution redox potential. Indeed, under a low negative applied bias (≥−0.3 V) the immobilized Cyt-*c* remains in the oxidised state (there is no absorption increase of the reduction bands) although its redox potential in solution is +38 mV *vs* Ag/AgCl. As the applied negative bias is further increased from −0.3 V Cyt-*c* is gradually reduced.

The fact that sometimes the commercial Cyt-*c* is significantly impure is not sufficient to explain the high negative potential required for its electrochemical reduction as similar reduction potentials were observed for immobilized Cyt-*c* whether commercial or purified.

Furthermore, the suggestion by some authors [25], that the electron transfer between the TiO_2 film and the immobilized proteins when applying a high negative potential (−0.7 V) is not direct due to reduction of hydrogen or oxygen at the TiO_2 electrode, is in this case contradicted by experimental evidence. In the course of the charging behaviour seen for blank TiO_2 films in the range of potentials investigated, very little current flows through the solution as is seen from the ratio of the integrated anodic and cathodic currents (minimal Faradic current) [26]. This is attributed to the fact that the buffer used is thoroughly purged of oxygen and it is not until significantly more negative potentials than those applied that reduction of protons occurs at TiO_2 [25]. This is strong evidence that the reduction of Cyt-*c* that is observed on the TiO_2 electrodes is the result of direct electron transfer from the TiO_2 electrode to the protein and not through the generation of either hydrogen peroxide or hydrogen at the electrode or because mediators or promoters were added.

The reduction potential for the immobilized Cyt-*c* on the TiO_2 films (−0.7 V) is thus due to the low conductivity of the TiO_2 electrode below its conduction band edge and at more positive potentials. This value can be tentatively attributed to the influence of the electrostatic charges at the TiO_2/solution interface. At the solution pH employed (pH 7), the surface of the TiO_2 is expected to be negatively charged [3,12], consistent with a negative shift of the protein reduction potential. Indeed, the change in pH of the electrolyte solution induces a ~−64 mV per pH unit shift on the potential of the reduction peak of the immobilized proteins and therefore the well-known dependence of the conduction band edge of TiO_2 films on pH (shifts of approximately −60 mV per pH unit [21]) was confirmed. The insulating region which results (at potentials positive of −0.3 V) because of the large band gap of the TiO_2 films also explains why scanning in the positive direction results in no peak due to protein re-oxidation.

Thus, at potentials at which Cyt-*c* would be expected to be oxidised it is well insulated by the TiO_2 film because the Fermi level of the film lies well within its bandgap and its conductivity is therefore very low. When the applied biases are in the range of −0.3 to −0.6 V, the adsorbed Cyt-*c* is getting reduced and the reduction kinetics are faster the higher the applied bias. Reduction should still in theory reach completion for potentials $< E_m$ (E_m defined as the mid-point potential) of the adsorbed protein. However it is noticed that this completion is not reached. The reasons could be that Cyt-*c* behaves differently due to either different conformation it takes after it is adsorbed, how exposed and in direct contact with the electrode the heme is, or be linked to variations in potential felt by the TiO_2 electrode. Indeed, how fast the electrons travel in the electrode and if they get trapped or not depends on the applied bias and therefore, if the applied bias is lower than −0.7 V, they are able to reduce some of the adsorbed Cyt-*c* molecules but not all of them.

This hypothesis is supported by the spectroelectrochemical experiments: the potential induced optical changes in nanostructured TiO_2 films are mainly due to the accumulation of electrons in conduction band states. Using this band filling model, it is possible to explain the observed spectra. At low negative applied potentials, up to −0.3 V, the optical absorption spectrum of a nanostructured TiO_2 film is the same as the one of an unbiased one. At more negative potentials a pronounced absorption maximum develops at 750 nm. This absorbance increase at 750 nm is assigned to intra- and interband transitions by electrons accumulated in conduction band states. When high negative potentials are applied to the TiO_2 electrodes electron accumulation and H^+ intercalation is accompanied by band filling according to the following equation:

$$Ti^{IV}O_2 + e^-(\text{external}) + H^+(\text{solution}) \rightarrow Ti^{III}O(OH)$$

That is, electrons occupy conduction band states with the accumulated charge being compensated by adsorption of a proton from the aqueous electrolyte [19,20].

Previous work [21] in addition to our own studies has shown that in aqueous buffer at pH 7 trap filling effects and electron accumulation in TiO_2 films takes place above −0.3 V. This is due to the large band gap (3.2 eV) for this material and explains why both of the proteins studied are reduced at more negative potentials than might be expected.

Spectroelectrochemical studies indicate that for all the coated and uncoated TiO_2 films, nearly all (>90%) of the immobilized Cyt-*c* is electrochemically reducible. However electrochemical reduction of the immobilized Cyt-*c* is observed only for potentials significantly negative of its solution phase mid-point potential of +0.038 V *vs* Ag/AgCl. Reduction peaks in the CVs are observed at −0.58 and −0.48 V for TiO_2 and SiO_2–TiO_2, respectively.

The use of TiO_2 films coated with silica rather than uncoated TiO_2 electrodes allows reduction of Cyt-*c* at less negative potentials, because of the greater conductivity when TiO_2 is coated with SiO_2. As described before [17], the TiO_2 conduction band can be shifted upwards when acidic species are adsorbed onto the nanoparticles. This shift increases the mesoporous TiO_2 film conductivity. On the other hand, basic coatings such as Al_2O_3 or MgO_2 do have the opposite effect and lower drastically the TiO_2 conductivity, which impedes the reduction of Cyt-*c* as illustrated in Fig. 7. In good agreement with this hypothesis are the results obtained for the zirconia coating (ZrO_2 is considered an acidic metal oxide, those PZC is very close to the one of TiO_2): the same negative potentials as for uncoated TiO_2 films lead to

the reduction of the adsorbed Cyt-*c*. On the other hand for all the other coatings more negative potentials (than for uncoated TiO_2 films) are necessary for the reduction of the immobilized protein. One can thus see a clear correlation between the Cyt-*c* reduction potential and the PZC of the coating of the titania electrode.

No protein oxidation peaks are observed in the CVs for all the coated or uncoated TiO_2 films. Re-oxidation of Cyt-*c* immobilized on all films, monitored spectroelectrochemically, is achieved only by the prolonged application of positive potentials (4–120 min). This is consistent with the essentially insulating behaviour of all materials for potentials positive of the protein mid-point potential, where the semiconductor Fermi level lies deep within the materials bandgap. We note that the prolonged application of moderate negative potentials to the coated or uncoated/Cyt-*c* does not result in complete reduction of the adsorbed protein, as monitored spectroelectrochemically (Figs. 7 and 8). This indicates that the influence of the coating overlayer on conductivity upon the protein reduction cannot be considered in terms of the macroscopic film conductivity alone. We note that for the potential range under consideration, charging of the coated or uncoated TiO_2 films, and, therefore, their electrical conductivity, are most probably dominated by sub-bandgap trap states. The spatial distribution of such states is likely to be microscopically heterogeneous, and may result in, at moderate applied potentials, only a subpopulation of the immobilized proteins being electrically accessible. However, at more negative potentials all of the film becomes effectively conductive and all of the adsorbed proteins may be reduced electrochemically, as is observed in Fig. 7.

5. Conclusions

In this paper the electrochemical properties of the mesoporous TiO_2 films were characterised. It is clearly demonstrated that the immobilized protein studied here retains its electrochemical activity, characterised by both UV/Vis spectroelectrochemistry and cyclic voltammetry. However, the TiO_2 films have an insulating region at low negative potentials and this is attributed to their limited conductivity at such potentials. Conformal overlayers of a range of metal oxides can be grown on porous nanocrystalline TiO_2 films by a solution chemistry approach under aerobic conditions. Our studies have investigated four different metal oxide overlayers on TiO_2:Al_2O_3, SiO_2, ZrO_2 and MgO_2. However, their influence on the reduction of the immobilized protein under applied biases is remarkably different, and can be linked to the PZC, and thus the surface charge, of the corresponding metal oxide. This pinpoints the influence of the surface charge as well as its structure on the design of new biosensors.

Acknowledgements

Financial support from BBSRC and ICREA is gratefully acknowledged. EP thanks the Spanish Ministerio de Ciencia e Innovacion for the CONSOLIDER-Hope 0007-2007 and the CTQ2007-60746/BQU projects.

References

[1] E. Topoglidis, A.E.G. Cass, G. Gilardi, S. Sadeghi, N. Beaumont, J.R. Durrant, Protein adsorption on nanocrystalline TiO_2 films: an immobilization strategy for bioanalytical devices, Anal. Chem. 70 (1998) 5111–5113.

[2] E. Topoglidis, T. Lutz, R.L. Willis, C.J. Barnett, A.E.G. Cass, J.R. Durrant, Protein adsorption on nanporous TiO_2 films: a novel approach to studying photoinduced protein/electrode transfer reactions, Faraday Discuss. 116 (2000) 35–46.

[3] E. Topoglidis, C.J. Campbell, A.E.G. Cass, J.R. Durrant, Factors that affect protein adsorption on nanostructured titania films. A novel spectroelectrochemical application to sensing, Langmuir 17 (2001) 7899–7906.

[4] E. Topoglidis, A.E.G. Cass, B. O'Regan, J.R. Durrant, Immobilisation and bioelectrochemistry of proteins on nanoporous TiO_2 and ZnO films, J. Electroanal. Chem. 517 (2001) 20–27.

[5] E. Topoglidis, Y. Astuti, F. Duriaux, M. Gratzel, J.R. Durrant, Direct electrochemistry and nitric oxide interaction of heme proteins adsorbed on nanocrystalline tin oxide electrodes, Langmuir 19 (2003) 6894–6900;
K. Poland, E. Topoglidis, J.R. Durrant, E. Palomares, Optical sensing of cyanide using hybrid biomolecular films, Inorg. Chem. Commun. 9 (2006) 1239–1242.

[6] C. Grealis, E. Magner, The oxidation of cytochrome *c* in nonaqueous solvents, Chem. Comm. 8 (2002) 816–817.

[7] Q. Li, G. Luo, J. Feng, Direct electron transfer for heme proteins assembled on nanocrystalline TiO_2 film, Electroanalysis 13 (2001) 359–363.

[8] C.A. Paddon, F. Marken, Hemoglobin adsorption into TiO_2 phytate multi-layer films: particle size and conductivity effects, Electrochem. Commun. 6 (2004) 1249–1253.

[9] K.R. Meier, M. Gratzel, Redox targeting of oligonucleotides anchored to nanocrystalline TiO_2 films for DNA detection, Chem. Phys. Chem. (2002) 371–374.

[10] J.K. Mbindyo, J.F. Rusling, Catalytic electrochemical synthesis using nanocrystalline titanium dioxide cathodes in microemulsions, Langmuir 14 (1998) 7027–7033.

[11] P. Cuendet, M. Gratzel, Light-induced reduction of cytochrome-*c* by colloidal TiO_2, Bioelectrochem. Bioenerg 16 (1986) 125–133.

[12] H. Shinohara, M. Gratzel, N. Vlachopoulos, M. Aizawa, Interfacial electron-transfer of flavin coenzymes and riboflavin adsorbed on textured TiO_2 films, Bioelectrochem. Bioenerg. 26 (1991) 307–320.

[13] E.V. Milsom, H.A. Dash, T.A. Jenkins, M. Opallo, F. Marken, The effects of conductivity and electrochemical doping on the reduction of methemoglobin immobilized in nanoparticulate TiO_2 films, Bioelectrochemistry 70 (2007) 221–227.

[14] M. Etienne, D. Grosso, C. Boissiere, C. Sanchez, A. Walcarius, Electrochemical evidences of morphological transformation in ordered mesoporous titanium oxide thin films, Chem. Commun. 36 (2005) 4566–4568.

[15] Z.P. Yang, S.H. Si, Y.S. Fung, Bilirubin adsorption on nanocrystalline titania films, Thin Solid Films 515 (2007) 3344–3351.

[16] C.J. Barbe, F. Arendse, P. Comte, M. Jirousek, F. Lenzmann, V. Shklover, M. Gratzel, Nanocrystalline titanium oxide electrodes for photovoltaic applications, J. Am. Ceram. Soc. 80 (1997) 3157–3171.

[17] E. Palomares, J.N. Clifford, S.A. Haque, T. Lutz, J.R. Durrant, Control of charge recombination dynamics in dye sensitized solar cells by the use of conformally deposited metal oxide blocking layers, J. Am. Chem. Soc. 125 (2003) 475–482.

[18] G. Rothenberger, D. Fitzmaurice, M. Grätzel, Optical electrochemistry .3. spectroscopy of conduction band electrons in transparent metal oxide semiconductor-films - optical determination of the flat-band potential of colloidal titanium-dioxide films, J. Phys. Chem. 96 (1992) 5983–5986.

[19] B. O'Regan, M. Graetzel, D. Fitzmaurice, Optical electrochemistry. 2. Real-time spectroscopy of conduction band electrons in a metal oxide semiconductor electrode, J. Phys. Chem. 95 (1991) 10525–10528.

[20] G. Boschloo, D. Fitzmaurice, Spectroelectrochemical investigation of surface states in nanostructured TiO_2 electrodes, J. Phys. Chem. B 103 (1999) 2228–2231.

[21] G. Boschloo, D. Fitzmaurice, Electron accumulation in nanostructured TiO_2 (anatase) electrodes, J. Electrochem. Soc. 147 (2000) 1117–1123.

[22] E. Stellwagen, Reversible unfolding of horse heart Ferricytochrome *c*, Biochemistry 7 (1968) 2893–2898.

[23] M. Kosmulski, Chemical Properties of Material Surfaces, Marcel Dekker, 2001.

[24] E. Stellwagen, Heme exposure as determinate of oxidation–reduction potential of heme proteins, Nature 275 (1978) 73–74.

[25] N. Serpone, I. Texier, A.V. Emeline, P. Pichat, H. Hidaka, J. Zhao, Post-irradiation effect and reductive dechlorination of chlorophenols at oxygen-free TiO_2/water interfaces in the presence of prominent hole scavengers, J. Photochem. Photobiol. A Chem. 136 (2000) 145–155.

[26] G. Boschloo, D. Fitzmaurice, Electron accumulation in nanostructured TiO_2 (anatase) electrodes, J. Phys. Chem. B. 103 (1999) 7860–7868.